高等学校化学学报
CHEMICAL JOURNAL OF CHINESE UNIVERSITIES
研究论文

一种具有荧光性质的阳离子Ga-MOF用于Fe^{3+}和硝基化合物识别

吴　季[1], 张　浩[1], 骆昱晖[1], 耿吴越[1], 兰亚乾[2]
(1. 江苏海洋大学环境与化学工程学院, 连云港 222000;
2. 华南师范大学化学学院, 广州 510631)

摘要　通过溶剂热法合成了一种新型阳离子镓金属-有机框架Ga-MOF, 其化学式为$[Ga_3O(H_2O)_3(TCA)_2]\cdot NO_3\cdot 6DMF\cdot 2H_2O$(JOU-27, H_3TCA=4,4′,4″-三苯胺三羧酸). 结构分析表明, JOU-27是基于氧心三核镓簇的三维微孔结构. 由于荧光配体H_3TCA的引入, JOU-27具有强的荧光发射强度, 因此可用于检测Fe^{3+}离子和硝基芳香族化合物. 结果表明, 其对Fe^{3+}的检出限低至2.22×10^{-6} mol/L(Stern-Volmer常数K_{SV}=52823 L/mol); 当硝基苯(NB)浓度仅为3.27×10^{-3} mol/L时, 荧光猝灭效率可达91%. 进一步的研究表明, JOU-27的猝灭性能可能与荧光共振能量转移(FRET)效应、激发光吸收竞争以及骨架激发态与硝基芳烃化合物之间的电子转移有关.

关键词　阳离子型金属-有机框架; 镓; 荧光识别; Fe^{3+}离子; 硝基芳烃化合物
中图分类号　O611　　**文献标志码**　A　　doi: 10.7503/cjcu20210617

A Microporous Cationic Ga(III)-MOF with Fluorescence Properties for Selective sensing Fe^{3+} Ion and Nitroaromatic Compounds

WU Ji[1], ZHANG Hao[1], LUO Yuhui[1*], GENG Wuyue[1], LAN Yaqian[2*]
(*1. School of Environmental and Chemical Engineering, Jiangsu Ocean University, Lianyungang* 222000, *China*;
2. School of Chemistry, South China Normal University, Guangzhou 510631, *China*)

Abstract　A new cationic gallium-organic framework, namely $[Ga_3O(H_2O)_3(TCA)_2]\cdot NO_3\cdot 6DMF\cdot 2H_2O$(JOU-27, H_3TCA=4,4′,4″-tricarboxyltriphenylamine), has been synthesized by solvothermal method and characterized. Structural analyses show that JOU-27 is a three-dimensional microporous framework based on oxygen-core trinuclear gallium clusters. Due to the introduction of fluorescent ligand, JOU-27 shows strong fluorescence emission and was developed as a fluorescent sensor to detect Fe^{3+} ion and nitroaromatic compounds. The detection limit of Fe^{3+} is as low as 2.22×10^{-6} mol/L(K_{SV}=52823 L/mol, K_{SV} is the Stern-Volmer constant). When the nitrobenzene(NB) concentration is only 3.27×10^{-3} mol/L, the quenching efficiency can reach 91%. In addition, further studies show that the quenching performance of JOU-27 may be due to the fluorescence resonance energy transfer(FRET) effect, the competition of excitation light absorption, and the electron transfer between the excited state of the framework and nitroaromatics.

Keywords　Cationic metal-organic framework; Gallium; Fluorescence sensing; Iron(III) ion; Nitroaromatic compound

收稿日期: 2021-08-25. 网络首发日期: 2021-10-11.
联系人简介: 骆昱晖, 男, 博士, 讲师, 主要从事晶态材料的设计合成研究. E-mail: luoyh@jou.edu.cn
兰亚乾, 男, 博士, 教授, 主要从事配位化学在清洁能源领域的应用研究. E-mail: yqlan@m.scnu.edu.cn
基金项目: 江苏省"六大人才高峰"高层次人才项目(批准号: XCL-009)和江苏省先进材料功能调控技术重点实验室开放基金(批准号: AM201902)资助.
Supported by the Six Talents Peak Project of Jiangsu Province, China(No. XCL-009) and the Open Project of the Jiangsu Key Laboratory of Function Control Technology for Advanced Materials, China(No.AM201902).

1 Introduction

Iron plays a very important role in human body and it can transport oxygen in the blood. However, abnormal iron content in the human body can cause various diseases, including anemia, skin diseases, insomnia, and so on[1]. Therefore, sensitive and specific detection of the content of Fe^{3+} is of great significance to the health of human[2]. On the other hand, nitroaromatic compounds(NACs) have hidden dangers in terms of environment and national security. They have the risk of explosion and endanger biological health. If the concentration of NACs exceeds a certain value in nature, it may cause serious harm to the human society[3]. Thus, it is also important to detect NACs simply and efficiently. At present, traditional molecular/ion detection techniques, including high performance liquid chromatography, inductively coupled plasma mass spectrometry, and atomic absorption spectrometry, have been applied for this purpose. However, these traditional detection methods have disadvantages such as complicated operations, inconvenient equipment, and high detection costs[4,5]. Therefore, it is very important to develop a rapid, convenient, and effective technology for detecting metal ions and NACs.

Metal organic frameworks(MOFs) are a new class of multifunctional porous materials with periodic structures assembled from metal ions(clusters) and organic ligands[6—10]. Since the chemical composition and surface environment of MOFs are finely tunable, they show the characteristics of easy functionalization. Due to these advantages, MOFs have been widely applied in magnetic materials, catalysis, photonics, gas storage/separation, and targeted drug transportation[11—18]. MOFs with fluorescence property have also been utilized as probe for metal ions or small molecules detection. Bu *et al.*[19] reported a Cd-MOF for detecting NACs, where the quenching phenomenon was mainly due to the electron transfer from the excited state of MOF framework to nitroaromatics. Li *et al.*[20] designed a Zn-MOF for sensitive and selective sensing Fe^{3+} ion in water. The competitive absorption between MOF and Fe^{3+} ion is the mainly reason for fluorescence quenching. These results reveal that fluorescent MOFs can be utilized as potential materials for sensing metal ions and NACs selectively. In particular, ionic MOFs have attracted increasing attention, because their charged framework may improve the host-guest interactions and then enhance their sensing properties[21]. Among the ionic MOFs, cationic MOFs with positively charged skeleton are widely used due to their high charge density and easy structure adjustment. Some synthesis strategies have been used to construct cationic MOFs. Firstly, when neutral ligands, such as 4,4′-bipyridine, are selected to coordinate with metal cations, and the coordination ability of anions is adjusted at the same time, cationic MOFs may be constructed[22]. Secondly, post-synthesis method is also an effective strategy for the preparation of cationic MOFs. For example, Cao *et al.*[23] designed a neutral MOF containing uncoordinated imidazole groups. Then, a cationic MOF was achieved through transforming the uncoordinated imidazole group into imidazolium salt. Recently, Bu *et al.*[24] proposed a new strategy to construct cationic MOFs, which is to introduce cationic clusters as secondary building units. In this strategy, the cationic clusters $[M_3O(COO)_6]^+$(M=Fe^{3+}, Al^{3+}, In^{3+}, Ga^{3+}…) are mostly investigated, because this kind of trinuclear clusters can be easily prepared. This strategy is efficient and has been used to construct many cationic MOFs. However, cationic MOFs based on trinuclear gallium clusters are relatively rarely studied[21].

Based on the above considerations, we aimed to design and construct cationic MOFs based on $[Ga_3O(COO)_6]^+$ clusters for metal ions and NACs detection. Herein, a newly cationic Ga-MOF was successfully synthesized using solvothermal method, namely $[Ga_3O(H_2O)_3(TCA)_2]\cdot NO_3\cdot 6DMF\cdot 2H_2O$(JOU-27, H_3TCA=4,4′,4″-tricarboxyltriphenylamine, DMF=*N*,*N*′-dimethylformamide). H_3TCA was chosen as ligand for its distinctive coordinate geometries and potential fluorescence properties. Structural analysis shows that JOU-27 is a three-dimensional(3D) microporous framework based on the oxygen-core trinuclear gallium

clusters. Due to the introduction of H_3TCA ligands, JOU-27 showed strong fluorescence emission and was developed as an efficient fluorescent sensor to detect Fe^{3+} ion and nitroaromatics. In addition, the quenching mechanism of JOU-27 has also been proposed. These results indicate that JOU-27 can be used as a multifunctional fluorescent probe for the detection of Fe^{3+} ions and NACs.

2 Experimental

2.1 Materials and Measurements

All reagents and solvents were purchased from commercial sources and used without purification. Powder X-ray diffraction (PXRD) patterns were collected on a PANalytical X'Pert Powder X-ray diffractometer with graphite monochromatized Cu $K\alpha$ radiation (λ=0.15418 nm), 2θ ranging from 5° to 50° with an increment of 0.02°/Step. The Fourier Transform infrared spectrophotometry (FTIR) spectra were measured by using KBr pellets in the range of 4000—400 cm^{-1} on a Thermo Scientific spectrometer. Thermogravimetric analysis (TGA) was performed on a Netzsch Thermal Analyzer (STA 449 F5) under N_2 atmosphere at a heating rate of 10 ℃/min. Brunauer-Emmett-Teller (BET) surface area of the samples was determined using N_2 adsorption/desorption technique (Micromeritics ASAP2020). The Ultraviolet-Visible (UV-Vis) absorption was measured with a PERSEE Ultraviolet-Visible-Near Infrared (UV-Vis-NIR) spectrophotometer. The fluorescent spectroscopy was measured on an FL-7000 Hitachi luminescence spectrometer at room temperature with a light source of Xenon lamp.

2.2 Synthesis of JOU-27

A mixture of $Ga(NO_3)_3 \cdot 9H_2O$ (0.032 mmol, 13.5 mg), H_3TCA (0.02 mmol, 7.5 mg), *N*,*N*-dimethylformamide (DMF, 1.5 mL) and HNO_3 (45 μL, 65%, mass fraction) was sonicated for 5 min, then transferred to a 10 mL pressure-resistant glass bottle and heated in an oven at 120 ℃ for 2 d. The light-yellow product was separated by filtration, washed with DMF and ethanol, and dried naturally. Yield: *ca.* 40% (calculated based on H_3TCA). Anal. calcd. for $C_{60}H_{76}Ga_3N_9O_{27}$ (%, found): C 46.06 (46.29), H 4.89 (4.62), N 8.06 (8.23). IR (KBr), $\tilde{\nu}$/cm^{-1}: 3430(s), 3030(m), 2778(m), 2427(w), 1627(m), 1598(m), 1506(w), 1463(m), 1385(s), 1321(m), 1280(w), 1182(w), 1070(w), 1018(w), 840(w), 784(w), 669(m), 540(m).

2.3 Metal Ions Sensing

The newly prepared JOU-27 was finely grounded into powder. Then, 3 mg of the obtained powder was immersed in 3 mL of DMF solution of different metal nitrates (1 mmol/L). The mixture was sonicated for 30 min and aged at room temperature for 24 h. Thereafter, the upper homogeneous dispersion was taken out for fluorescence spectrum test. In the fluorescence spectrum test experiment, the excitation wavelength was set to 340 nm and the fluorescent spectrum was monitored in the range of 360—600 nm.

2.4 Organic Molecules Sensing

The organic solvents were diluted with DMF to a concentration of 0.025 mol/L. Then, 10 μL of the diluted solutions were respectively added to the dispersion of JOU-27 (prepared by the same method shown in section 2.3). Under the excitation wavelength of 340 nm, the fluorescent spectra of the dispersion were monitored in the range of 360—600 nm.

3 Results and Discussion

3.1 Structure of JOU-27

Powder crystalline products of JOU-27 were synthesized through a solvothermal process. Pawley refinements of the PXRD data of JOU-27 revealed an isostructure identical to the reported MOFs, but with slightly

different unit cell parameters (Fig. S1 and Table S1, see the Supporting Information of this paper)[25]. As shown in Fig. S2 (see the Supporting Information of this paper), there are six crystallography independent Ga(III) ions, four TCA^{3-} ligands and six coordination water molecules in the asymmetric unit of JOU-27. As shown in Fig. 1(A), Ga(III) ions are six-coordinated by four carboxylate oxygen atoms, one μ_3-oxygen atom and one water oxygen atom, giving a distorted octahedral geometry. Then, three Ga(III) ions are connected to form a $[Ga_3O(COO)_6]^+$ cluster. Thanks to the TCA^{3-} ligands, the trimeric clusters are connected into a 3D microporous framework [Fig. 1(B)—(D)]. Topologically, each trimeric cluster linking to six TCA^{3-} can be defined as a six-connected node, whereas each TCA^{3-} ligand coordinating to three trimeric clusters can be defined as a three-connected node. Then, the framework of JOU-27 can be reduced to (3, 6)-connected network with Schläfli symbol of $(6^6)(6^{15})$ [Fig. 1(D)]. Inspecting into the framework, all the microporous channels interconnecting inside the framework results in the 3D sinuous pores [Fig. 1(E)]. The total potential solvent-accessible volume of JOU-27 was calculated to be 68.5% using PLATON program[26]. On the basis of the calculated crystal model and the results of thermogravimetric analysis and elemental analysis, a molecular formula of $[Ga_3O(H_2O)_3(TCA)_2]\cdot NO_3\cdot 6DMF\cdot 2H_2O$ was obtained for JOU-27. Nitrate ion, which cannot be determined from structural refinement, was added to the formula directly to balance the charge.

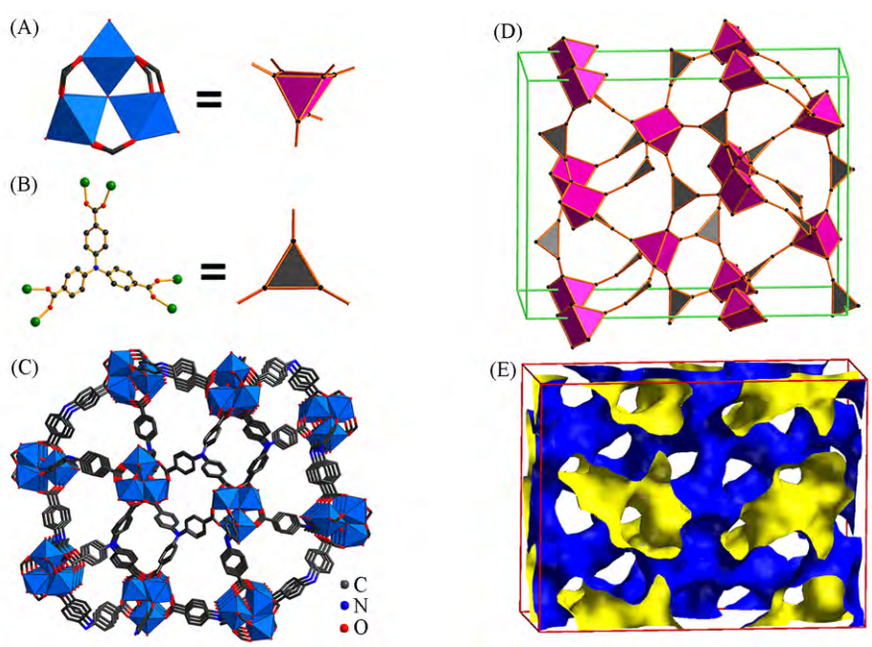

Fig. 1 Polyhedral representation of $[Ga_3O(COO)_6(H_2O)_3]^+$ unit(A), coordination model of TCA^{3-} ligand(B), view of the 3D porous framework of JOU-27(C), topological structure of JOU-27(D) and connolly surface of the porous structure of JOU-27(E)

(E) Created with a spherical probe with 0.16 nm radius; blue internal and yellow external.

3.2 Characterizations

First, the purity of the product was confirmed using PXRD technique. As shown in Fig. S3 (see the Supporting Information of this paper), the PXRD pattern of as-synthesized JOU-27 is consistent well with the simulated one, indicating the high phase purity of the synthesized sample. The porosity of JOU-27 was proven by N_2 adsorption-desorption analysis performed at 77 K (Fig. 2). Prior to sorption analysis, the sample was activated by heating at 120 ℃ under dynamic vacuum. The N_2 adsorption-desorption isotherms show a typical type IV isotherm with pronounced adsorption-desorption hysteresis, indicating the existence of micropores and mesopores in the sample. The calculated BET surface area is 453.1 m^2/g. The TGA result reveals that JOU-27 exhibits a conspicuous solvent mass loss of about 30.2% (calculated 30.3%) from 45 to 230 ℃, which

confirms its highly porous structure (Fig. S4, see the Supporting Information of this paper). Thereafter, a further mass loss starts at about 300 ℃, which may be due to the decomposition of the framework. In the FTIR spectrum of JOU-27 (Fig. S5, see the Supporting Information of this paper), the strong and broad absorption band centered at about 3430 cm^{-1} may be due to the O—H vibrations of water molecules, the weak bands at about 3030 cm^{-1} is attributed to the stretching vibrations of Ar—H, whereas the strong bands at about 1627 and 1463 cm^{-1} indicate the presence of carboxylate groups.

The solid-state fluorescence properties of JOU-27 were studied at room temperature. As shown in Fig. 3, the emission peak of JOU-27 is at about 429 nm, which is almost unchanged compared with that of H_3TCA (426 nm). Therefore, the emission of JOU-27 is mainly derived from the fluorescence of the ligands[27—30]. Good fluorescence property of JOU-27 makes it a potential fluorescent sensor.

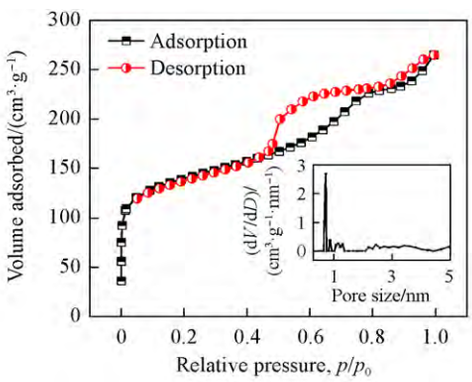

Fig. 2 N_2 adsorption-desorption isotherms of JOU-27 with pore size distribution curve(inset)

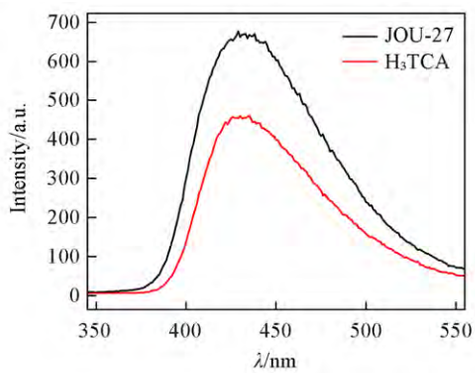

Fig. 3 Solid-state emission spectra of JOU-27 and H_3TCA(excited at 340 nm)

3.3 Sensing of Fe^{3+} Ion

The sensing performance of JOU-27 toward metal ions recognition is explored. Sixteen metal ions were selected for sensing research, they are K^+, Na^+, Ag^+, Mg^{2+}, Ca^{2+}, Ba^{2+}, Cu^{2+}, Co^{2+}, Cd^{2+}, Zn^{2+}, Pb^{2+}, Ni^{2+}, Mn^{2+}, Cr^{3+}, Fe^{3+} and Al^{3+}. Firstly, a certain amount of different metal ions (1 mmol/L) was added to the JOU-27 dispersion. It was found that only when Fe^{3+} was added, the fluorescence intensity of JOU-27 was significantly quenched, while other metal ions could not quench the emission of MOF solution (Fig. S6, see the Supporting Information of this paper). These results indicate that JOU-27 can be used to selectively recognize Fe^{3+} ion. Thereafter, the effect of Fe^{3+} concentration on the quenching effect of JOU-27 was studied. It can be seen from Fig. 4 that as the concentration of Fe^{3+} increases, the emission peak intensity of JOU-27 decreases. The relationship between the emission peak intensity of JOU-27 and Fe^{3+} ion concentration can be fitted as I_0/I=0.9479+53823[Fe^{3+}] (R^2=0.9845). This is consistent with the Stern-Volmer equation: $I_0/I=1+K_{SV}[M]$[31], where I_0 and I represent the emission peak intensity of JOU-27 before and after the addition of metal ions, respectively; [M] indicates the molar concentration of Fe^{3+}; K_{SV} (L/mol) is the Stern-Volmer constant. The limit of detection (LOD) of JOU-27 toward

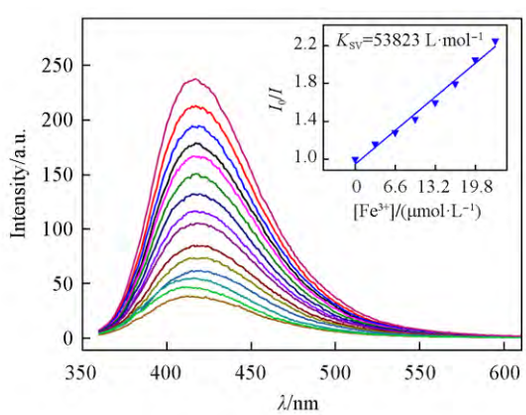

Fig. 4 Emission spectra of JOU-27 in DMF solution with different concentrations of Fe^{3+}

[Fe^{3+}]/(μmol·L^{-1}) from top to bottom: 0, 3.3, 6.6, 10, 13.3, 16.6, 20, 23.3, 26.6, 30, 33.3, 36.6, 40, 60, 80. Inset: the Stern-Volmer plots of JOU-27 dispersed in different concentrations of Fe^{3+} solutions.

Fe^{3+} ion is calculated to be 2.22×10^{-6} mol/L using the formula $LOD=3s/K_{SV}$, where s is the standard deviation of blank[32]. The LOD of JOU-27 is comparable to other reported MOF materials and the comparison is shown in Table S2(see the Supporting Information of this paper). The sensing selectivity of JOU-27 was also investigated. It can be seen from Fig.S7(see the Supporting Information of this paper) that when the same amount of other 15 metal ions (except Fe^{3+}) is added, the emission intensity of JOU-27 dispersion hardly changes. However, after adding the same amount of Fe^{3+} solution, the emission intensity of JOU-27 dispersion shows obvious quenching phenomenon. These results indicate that JOU-27 can be used as a fluorescent "turn-off" sensor to selectively detect Fe^{3+} ion.

3.4 Mechanism for Fe^{3+} Ion Sensing

The quenching mechanism of JOU-27 in the presence of Fe^{3+} was proposed through the following experiments. Firstly, the fresh prepared JOU-27 was immersed in a DMF solution containing Fe^{3+}(0.1 mmol/L) for 24 h. The sample was filtered out and analyzed by PXRD technique. The PXRD pattern of Fe^{3+}@JOU-27 is consistent with that of the as-synthesized JOU-27, indicating that the MOF was not collapsed[Fig.5(A)]. Secondly, the response time of fluorescence quenching is less than 5 s, revealing that there is almost no ion exchange between JOU-27 and Fe^{3+} during the sensing process[33—35]. Thereafter, the UV-Vis absorption spectra of the mixture of JOU-27 and Fe^{3+} were tested. It is found that in addition to the characteristic peak of Fe^{3+} and JOU-27, there is no new absorption peak(Fig.S7), which indicates that no charge transfer occurs between them. On the other hand, the absorption band of Fe^{3+} ions significant covers the emission band of JOU-27, revealing that the fluorescence resonance energy transfer(FRET) effect may be a reason for the quenching phenomenon of JOU-27 in the presence of Fe^{3+}[Fig.5(B)]. In addition, the absorption bands of JOU-27 and Fe^{3+} partially overlap, leading to the competition of excitation energy absorption(Fig.S8, see the Supporting Information of this paper)[36]. Therefore, the quenching phenomenon of JOU-27 in the presence of Fe^{3+} can be attributed to the FRET effect and the competitive absorption of excitation light[37].

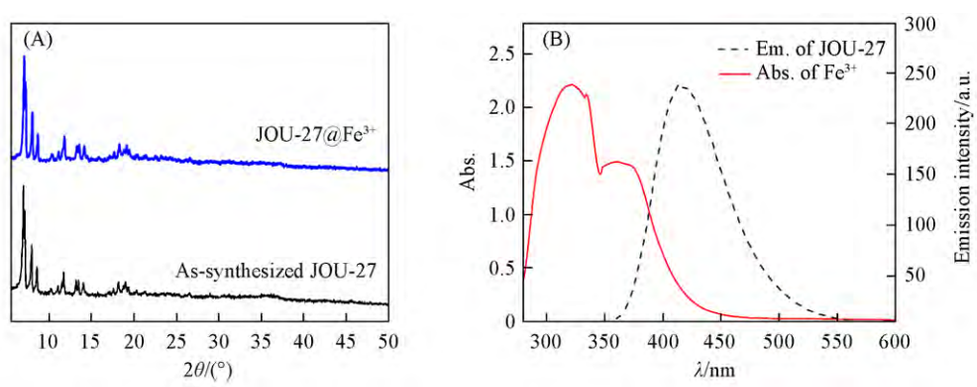

Fig. 5 PXRD patterns of JOU-27 before and after immersing in Fe^{3+} DMF solution(A) and UV-Vis absorption spectrum of Fe^{3+} DMF solution and emission spectrum of JOU-27(B)

3.5 Sensing of Nitroaromatic Compounds

The sensing performance of JOU-27 toward NACs was also studied. Sixteen different organic solvents were selected for solvent identification research, they are acetone, dichloromethane, chloroform, dimethyl sulfoxide, 1, 4-dioxane, cyclohexane, tetrahydrofuran, isopropyl alcohol, ethanol, acetonitrile, ethyl acetate, methanol, ether, toluene, ethylene glycol and nitrobenzene(NB). Fluorescence spectra in Fig.S9 (see the Supporting Information of this paper) show that only NB can quench the emission of JOU-27. Therefore, JOU-27 can be utilized as a fluorescent probe for selective recognition of NB. Then, the quenching effect of NB concentration on the emission of JOU-27 was studied. When 0.5 μL of 0.025 mol/L NB solution

was added into 3 mL of JOU-27 dispersion, the quenching efficiency can reach 12.39% within a few seconds [Fig.6(A)]. These results show that JOU-27 has excellent sensitivity and rapid response for NB sensing. When 100 μL of 0.025 mol/L NB solution was added, the emission peak of JOU-27 dispersion was significantly quenched(60.3%). Subsequently, the relationship between emission intensity of JOU-27 and the concentration of NB was investigated. As the concentration of NB increases, the emission intensity of JOU-27 gradually decreases. The relationship between the emission intensity of JOU-27 and the concentration of NB can be fitted as I_0/I = 0.9685 + 30907[NB](R^2=0.996)[Inset of Fig.6(A)]. This result is consistent with the Stern-Volmer equation: I_0/I=1+K_{SV}[M][31], where I_0 and I represent the emission peak intensity of JOU-27 before and after adding NB solution, and [M] is the concentration of NB. The quenching performance of JOU-27 is comparable to other reported MOF materials and the comparison is shown in Table S3(see the Supporting Information of this paper). The selectivity of JOU-27 toward NB sensing was also investigated. When the same amount of other organic solvents(except NB) is added, the emission intensities of JOU-27 dispersions show almost no change(Fig.S10, see the Supporting Information of this paper). However, after adding the same amount of NB, the emission intensity of JOU-27 dispersion is significantly quenched. These results reveal that JOU-27 can be used as a fluorescence probe for NB sensing.

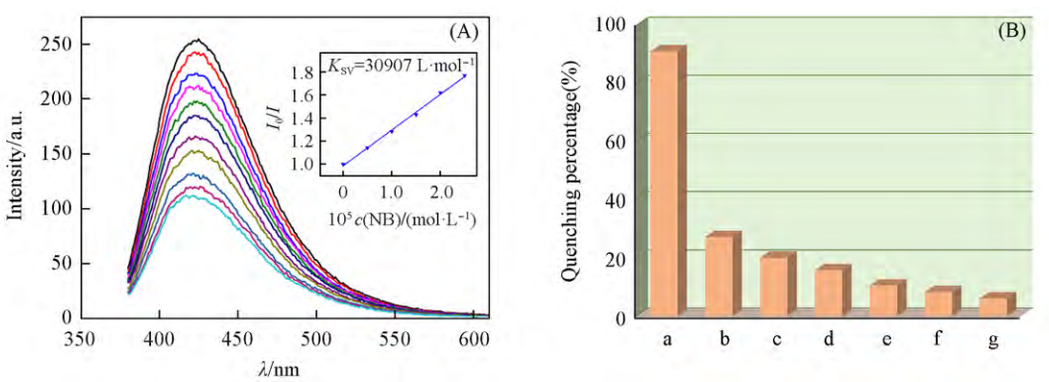

Fig. 6 Emission spectra of JOU-27 in DMF(3 mL) with different volume of NB solution(0.025 mol/L)(A) and quenching percentage of peak intensity of JOU-27 in the presence of different NACs(B)

Inset in (A): the Stern-Volmer plots of JOU-27 dispersed in the presence of different concentrations of NB.
(A) Volume of NB solution/μL from top to bottom: 0, 10, 20, 30, 40, 50, 60, 70, 80, 90, 100.
(B) a. NB; b. 4-NP; c. 4-NA; d. 4-NT; e. 3-NAP; f. 4-NCB; g. 4-NAP.

Interestingly, JOU-27 also can be used as a fluorescence probe for sensing other nitroaromatics. The corresponding fluorescence changes of the emulsion were monitored by fluorescence spectroscopy upon incremental addition of DMF solutions of nitroaromatics, including 4-nitrophenol (4-NP), 4-nitroacetophenone (4-NAP), 4-nitroaniline(4-NA), 4-nitrophenol(4-NP), 4-nitrotoluene(4-NT), *m*-nitroacetophenone(3-NAP) and 4-nitrochlorobenzene(4-NCB). When the concentration of different nitroaromatics in JOU-27 dispersion reaches 3.27×10^{-3} mol/L, the order of quenching efficiency is NB(91%)>4-NP(27.18%)>4-NA(20.06%)>4-NT(15.8%)>3-NAP(10.51%)>4-NCB 8.25%)>4-NAP(6.01%)[Fig.6(B)], indicating that JOU-27 can be used as a fluorescent probe for sensing nitroaromatics.

3.6 Mechanism for Nitroaromatic Compounds Sensing

The following experiments were carried out to propose the fluorescence quenching mechanism of JOU-27 in the presence of NACs. Firstly, JOU-27 was immersed in NB DMF solution(0.025 mmol/L, in DMF) for 24 h, and then the powder was filtered out and analyzed by PXRD. As shown in Fig.7(A), JOU-27 is stable upon immersing in NB solution, indicating that the quenching phenomenon is not caused by the collapse of the framework. Because the absorption band of JOU-27 partially overlaps the absorption band of NACs, excitation

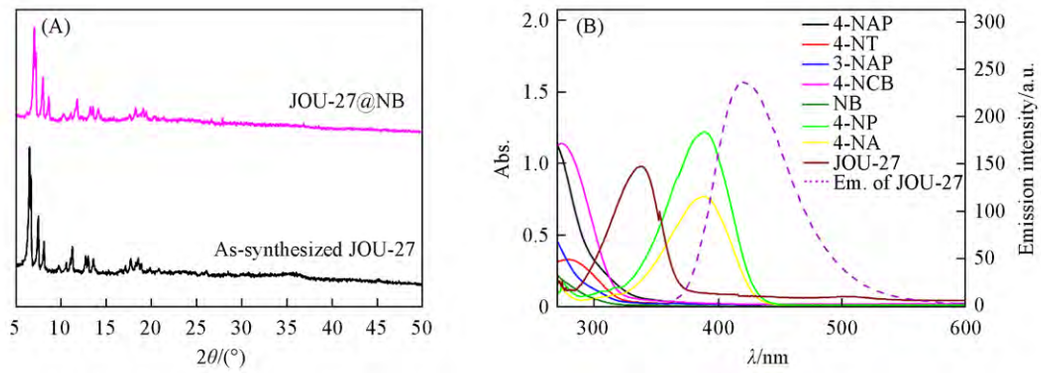

Fig. 7 PXRD patterns of JOU-27 before and after immersing in NB DMF solution(A) and UV-Vis absorption spectra of NACs' DMF solution and JOU-27 dispersion and emission spectra of JOU-27(B)

light absorption competition may also occur[38]. In order to verify whether there exists FRET between JOU-27 and analytes, the UV-Vis spectra were tested. As shown in Fig.7(B), only the absorption bands of 4-NA and 4-NP partially cover the emission band of JOU-27, indicating that emission light of JOU-27 may be absorbed by 4-NA and 4-NP[39]. Therefore, both the competition of excitation light absorption in the presence of NACs and the FRET effect may cause the emission quenching of JOU-27. On the other hand, due to the electron withdrawing properties of nitroaromatics, the electron transfer may also occur from the excited state of electron-donating framework of JOU-27 to NACs, leading to quenching phenomenon[40,41].

4 Conclusions

A three-dimensional cationic Ga-MOF(JOU-27) with cross-linked microporous channels was constructed by simple solvothermal method. Structural analyses show that the framework of JOU-27 is based on trinuclear gallium clusters. Due to the introduction of triphenylamine based ligand, JOU-27 showed strong emission when it was dispersed in DMF solution. Based on this, JOU-27 was developed as an efficient fluorescence "turn-off" sensor to detect Fe^{3+} and nitroaromatic compounds. For Fe^{3+} detection, the K_{SV} is as high as 53823 L/mol, and the detection limit is 2.22×10^{-6} mol/L. For nitroaromatics sensing, good quenching efficiency was also obtained, indicating that JOU-27 has good detection ability for these nitroaromatics, especially for NB. When the concentration of NB is as low as 3.27×10^{-3} mol/L, the quenching efficiency can reach 91%. Further research found that the fluorescence quenching may be due to the FRET effect, the competition of excitation light absorption, and the electron transfer between the excited state of MOF framework and nitroaromatics. These results indicate that JOU-27 can be used as a multifunctional material for the detection of Fe^{3+} ion and nitroaromatic compounds.

The supporting information of this paper see http://www.cjcu.jlu.edu.cn/CN/10.7503/cjcu20210617.

References

[1] Tümay S. O., Irani-nezhad M. H., Khataee A., *J. Photoch. Photobio. A*, **2020**, *402*, 112819
[2] Carter K. P., Young A. M., Palmer A. E., *Chem. Rev.*, **2014**, *114*(8), 4564—4601
[3] Wu Y., Li Y., Zou L., Feng J., Wu X., *J. Coord. Chem.*, **2017**, *70*(6), 1077—1088
[4] Qu X. L., Gui D., Zheng X. L., Li R., Han H. L., Li X., Li P. Z., *Dalton Trans.*, **2016**, *45*(16), 6983—6989
[5] Ngue C. M., Leung M. K., Lu K. L., *Inorg. Chem.*, **2020**, *59*(5), 2997—3003
[6] Cui Y., Zhang J., He H., Qian G., *Chem. Soc. Rev.*, **2018**, *47*(15), 5740—5785
[7] Pascanu V., González M. G., Inge A. K., Martín-Matute B., *J. Am. Chem. Soc.*, **2019**, *141*(18), 7223—7234
[8] Du D. Y., Qin J. S., Li S. L., Su Z. M., Lan Y. Q., *Chem. Soc. Rev.*, **2014**, *43*(13), 4615—4632
[9] Jin J., Xue J. J., Liu Y. C., Yang G. P., Wang. Y. Y., *Dalton Trans.*, **2021**, *50*(6), 1950—1972

[10] Zhang W. H., Ren Z. G., Lang J. P., *Chem. Soc. Rev.*, **2016**, 45(18), 4995—5019
[11] Yan X., Li P., Song X., Li J., Ren B., *Coord. Chem. Rev.*, **2021**, *443*, 214034
[12] Wang B., Liu B., Yan Y., *J. Anal. Chem.*, **2021**, *76*(4), 430—441
[13] Wang J. H., Li M. N., Yan S., Zhan Y., Liang C. C., *Inorg. Chem.*, **2020**, *59*(5), 2961—2968
[14] Zirak H. K. S., Ghaee A., Farokhi M., Nourmohammadi J., Bahi A., *Int. J. Biol. Macromol.*, **2021**, *173*, 351—365
[15] Liu D., Lang J. P., Abrahams B. F., *J. Am. Chem. Soc.*, **2011**, 133(29), 11042—11045
[16] Liu C. Y., Chen X. R., Chen H. X., Niu Z., Hirao H., Braunstein P., Lang J. P., *J. Am. Chem. Soc.*, **2020**, 142(14), 6690—6697
[17] Shi Y. X., Zhang W. H., Abrahams B. F., Braunstein P., Lang J. P., *Argew. Chem. Int. Ed.*, **2019**, 58(28), 9453—9458
[18] Lei H., Zhang X., Jin J., Wang S., Ding S., Zhang N., Chen C., *Chem. Res. Chinese Universities*, **2020**, 36(5), 946—954
[19] Tian D., Li Y., Chen R. Y., Chang Z., Wang G. Y., Bu X. H., *J. Mater. Chem. A*, **2014**, *2*(5), 1465—1470
[20] Hou B. L., Tian D., Liu J., Dong L. Z., Li S. L., Li D. S., Lan Y. Q., *Inorg. Chem.*, **2016**, *55*(20), 10580—10586
[21] Karmakar A., Desai A. V., Ghosh S. K., *Coordin. Chem. Rev.*, **2016**, *307*(Pt2), 313—341
[22] Manna B., Chaudhari K. A., Joarder B., Karmakar A., Ghosh K. S., *Angew. Chem. Int. Ed.*, **2013**, *52*(3), 998—1002
[23] Liang J., Chen R. P., Wang X. Y., Liu T. T., Wang X. S., Huang Y. B., Cao R., *Chem. Sci.*, **2017**, *8*(2), 1570—1575
[24] Mao C., Kudla R. A., Zuo F., Zhao X., Mueller J. L., Bu X., Feng P., *J. Am. Chem. Soc.*, **2014**, *136*(21), 7579—7582
[25] Dong L. Z., Zhang L., Liu J., Huang Q., Lu M., *Angew. Chem. Int. Ed.*, **2020**, *59*(7), 2659—2663
[26] Spek A., *Acta Crystallogr., Sect. D: Biol. Crystallogr.*, **2009**, *65*(Pt2), 148—155
[27] Ni M., Gong M., Li X., Gu J., Li B., *Appl. Mater. Today*, **2021**, *23*, 100982
[28] Zhang H., Geng W. Y., Luo Y. H., Ding Z. J., Wang Z. X., Xie A. D., Zhang D. E., *CrystEngComm*, **2021**, *23*(18), 3319—3325
[29] Zhang H., Wu J., Geng W. Y., Luo Y. H., Ding Z. J., Wang Z. X., Zhang D. E., *J. Solid State Chem.*, **2021**, *302*, 122424
[30] Qian B., Chang Z., Bu X. H., *Chem. Res. Chinese Universities*, **2020**, *36*(1), 74—80
[31] Wang G. D., Li Y. Z., Shi W. J., Zhang B., Hou L., *Sensor Actuat. B-Chem.*, **2021**, *331*, 129377
[32] Gao L., Jiao C., Chai H., Ren Y., Zhang G., *J. Solid State Chem.*, **2020**, *284*, 121199
[33] Pan Y., Wang J., Guo X., Liu X., Tang X., *J. Colloid Interface Sci.*, **2018**, *513*, 418—426
[34] Du J. L., Zhang X. Y., Li C. P., Gao J. P., Hou J. X., Jing X., Mu Y. J., Li L. J., *Sensor Actuat. B-Chem.*, **2018**, *257*, 207—213
[35] Lv R., Chen Z., Fu X., Yang B., Li H., Su J., Gu W., Liu X., *J. Solid State Chem.*, **2018**, *259*, 67—72
[36] Chen H., Fan P., Tu X., Min H., Yu X., *Chem. Asian J.*, **2019**, *14*(20), 3611—3619
[37] Li X., Tang J., Liu H., Gao K., Meng X., *Chem. Asian J.*, **2019**, *14*(20), 3721—3727
[38] Shi D., Yang X., Chen H., Ma Y., Schipper D., Jones R. A., *J. Mater. Chem. C.*, **2019**, *7*(3), 13425—13431
[39] Chen T. C., Tsai M. J., Wu J. Y., *Chem. Eur. J.*, **2019**, *25*(5), 1337—1344
[40] Li Y., Liu K., Li W. J., Guo A., Zhao F. Y., Liu H., Ruan W. J., *J. Phys. Chem. C*, **2015**, *119*(51), 28544—28550
[41] Zheng H., Deng Y. K., Ye M. Y., Xu Q. F., Kong X. J., *Inorg. Chem.*, **2020**, *59*(17), 12404—12409

(Ed.: L, H, W, M)